Antiferromagnetic long-range order in dissipative Rydberg lattices

Michael Hoening,[1] Wildan Abdussalam,[2] Michael Fleischhauer,[1] and Thomas Pohl[2]

[1]*Fachbereich Physik und Forschungszentrum OPTIMAS, Technische Universität Kaiserslautern, D-67663 Kaiserslautern, Germany*
[2]*Max Planck Institute for the Physics of Complex Systems, Nöthnitzer Straße 38, D-01187 Dresden, Germany*

We study the dynamics of dissipative spin lattices with power-law interactions, realized via few-level atoms driven by coherent laser-coupling and decoherence processes. Using Monte Carlo simulations, we determine the phase diagram in the steady state and analyze its generation dynamics. As opposed to mean-field predictions and nearest-neighbor models, there is no transition to long-range-ordered phases for realistic interactions and resonant driving. However, for finite laser detunings, we demonstrate the emergence of crystalline order. Although the static and dynamical critical exponents of the revealed dissipative phase transition fall into the two-dimensional Ising universality class, the found steady states differ considerably from those of an equilibrium Ising magnet. Two complementary schemes for an experimental implementation with cold Rydberg atoms are discussed.

Experiments with cold atoms offer unique insights into many-body physics [1]. Measurement techniques have reached spatiotemporal resolution [2] that—combined with tunable zero-range interactions—are opening the door for microscopic observations of many-body dynamics. Laser excitation of Rydberg states adds strong and long-range interactions to this toolbox [3], being key to the exploration of new ordered phases with ultracold atoms [4]. One avenue is to prepare such phases as many-body ground states of a Hamiltonian via slow changes of laser frequency and/or intensity [5–7]. This requires sufficient time to remain adiabatic, which poses a challenging competition with the finite lifetime of the Rydberg states. Alternatively, the excited-state decay can also be employed as a natural means for the preparation of states [8]. The nonequilibrium physics of such driven open systems and its relation to universal behavior in equilibrium [9] has recently attracted considerable interest [10–13]. We show here that driven Rydberg gases are ideal systems to experimentally access nonequilibrium steady-state phase transitions.

Previous work considered lattices of effective spins, represented by an atomic ground and strongly interacting Rydberg state coupled by external laser driving and spontaneous decay [8,14,15]. The emergence of steady states with antiferromagnetic (AF) order was predicted on the basis of mean-field theory assuming nearest-neighbor (NN) interactions [8]. It was later shown, however, that ordering in these systems is restricted to short length scales for all spatial lattice dimensions due to large single-site fluctuations associated with a simple two-level driving scheme [15]. Simulations moreover showed that crystallization in one dimension (1D) is also precluded for other driving schemes [15], for which long-range order was predicted using mean-field theory [16]. Hence, the possibility of long-range order in dissipative Rydberg lattices as well as the physics of the associated phase transition have thus far remained an open question.

Here we address this issue and show that long-range-ordered antiferromagnetic phases can indeed be realized in dissipative Rydberg lattices when subject to appropriate coherent driving. However, fluctuations as well as the weak tail of the rapidly decaying interactions are both found to be essential. This stands in marked contrast to the equilibrium physics of the corresponding unitary systems, which often is well described by mean-field models [17] and NN approximations [18]. While the crystalline state strongly deviates from that of an equilibrium Ising magnet, the critical exponents of the nonequilibrium transition are found to be those of the Ising universality class.

The unitary evolution is governed by the general Hamiltonian

$$\hat{H} = \sum_i \hat{H}_i - \hbar\Delta \sum_i \hat{\sigma}_{\rm ee}^{(i)} + V_0 \sum_{i<j} \frac{\hat{\sigma}_{\rm ee}^{(i)}\hat{\sigma}_{\rm ee}^{(j)}}{|\mathbf{r}_i - \mathbf{r}_j|^\alpha}, \qquad (1)$$

for laser-driven atoms on a quadratic lattice of length L. The local Hamiltonian $\hat{H}_i$ describes the atom-light interaction that excites Rydberg states with a frequency detuning Δ and $\hat{\sigma}_{\rm ee}^{(i)}$ denotes the corresponding projector onto the Rydberg state of an atom at site $\mathbf{r}_i = (x_i,y_i)$, $x_i,y_i \in [1,L]$. We will discuss two specific examples (see Fig. 1) for $\hat{H}_i$ later on. The last term accounts for the Rydberg-Rydberg interaction, where $V_0 = C_\alpha/a^\alpha$ is the nearest-neighbor coupling for a lattice constant a and an interaction strength $C_\alpha > 0$. Dipole-dipole interactions correspond to $\alpha = 3$ and van der Waals (vdW) interactions to $\alpha = 6$. In addition, we consider Markovian loss and dephasing processes described by a suitable Lindblad operator $\hat{\mathcal{L}}[\rho]$ such that the N-body density matrix evolves as $\dot{\rho} = -i[\hat{H},\rho] + \hat{\mathcal{L}}[\rho]$.

Independent on the specific form of $\hat{H}_i$, the quantum dynamics can be reduced to the diagonal elements of ρ for sufficiently strong decoherence upon adiabatic elimination of its coherences and neglecting multiphoton excitation of two or more atoms [15,19–23].[1] This simplifies the time evolution to an effective classical rate equation model for the joint probabilities $\rho_{S_1,...,S_N}$ of Rydberg excitations being present ($S_i = 1$) or not present ($S_i = 0$) at the ith site. The corresponding many-body states are connected by single-atom excitation [$\Gamma_\uparrow(\delta_i)$] and deexcitation [$\Gamma_\downarrow(\delta_i)$] rates,

$$\dot{\rho}_{S_1,...,S_N} = \sum_i [(1-S_i)\Gamma_\downarrow(\delta_i) + S_i\Gamma_\uparrow(\delta_i)]\rho_{S_1,...,1-S_i,...,S_N}$$
$$- [(1-S_i)\Gamma_\uparrow(\delta_i) + S_i\Gamma_\downarrow(\delta_i)]\rho_{S_1,...,S_i,...,S_N}, \quad (2)$$

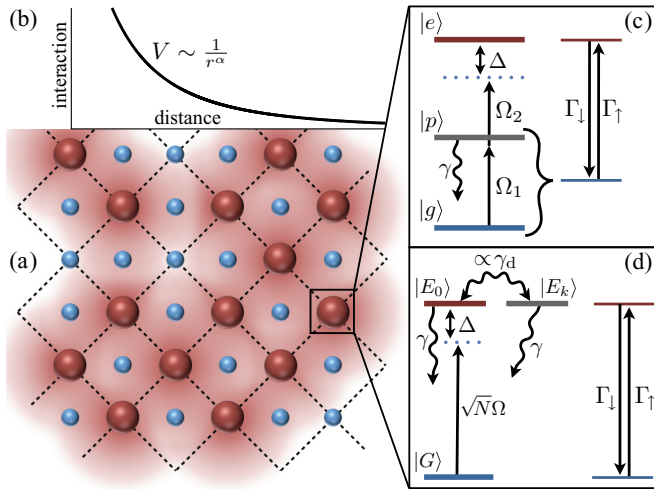[1]We have confirmed these simplifications via quantum simulations of smaller lattices.

FIG. 1. (Color online) (a) Schematics of a two-dimensional lattice in which ground-state atoms (small blue spheres) are laser excited to Rydberg states (large red spheres). The interplay of dissipation and Rydberg-Rydberg interactions (b) can give rise to antiferromagnetic long-range order, where excitations predominantly occupy one checkerboard sublattice. Two possible realizations of such effective two-level systems with tunable excitation rates $\Gamma_\uparrow$ and $\Gamma_\downarrow$ are illustrated in (c) and (d) (see text for details).

where the interactions enter through an effective frequency detuning $\delta_i = \Delta - V_0 \sum_{j \neq i} S_j |\mathbf{r}_i - \mathbf{r}_j|^{-\alpha}$ that accounts for the level shift of the ith atom due to its surrounding Rydberg excitations.

The steady-state single-particle probabilities can always be expressed as a simple Lorentzian,

$$\bar{\rho}_i(\delta_i) = \frac{\Gamma_\uparrow}{\Gamma_\uparrow + \Gamma_\downarrow} = \frac{p_0}{1 + \delta_i^2/\omega^2}. \quad (3)$$

The resonant excitation probability p_0 and linewidth ω depend on the excitation scheme (cf. Fig. 1) and will be given later. Together with the relaxation time $T(\delta_i)$ for a single lattice site, the rates in Eq. (2) can then be expressed as $\Gamma_\downarrow(\delta_i) = (1 - \bar{\rho}_i)/T$, $\Gamma_\uparrow(\delta_i) = \bar{\rho}_i/T$.

The formulation in terms of coupled N-body rate equations permits an efficient numerical treatment of large systems via kinetic Monte Carlo simulations [24]. We have performed dynamic Monte Carlo (dMC) based on the rates $\Gamma_{\uparrow(\downarrow)}$ and steady-state Monte Carlo (ssMC), assuming $T(\delta) = T = $ const, and found good agreement in the relevant parameter regimes. In the latter case, the many-body steady state is determined by only four parameters: p_0, the exponent α, the scaled detuning Δ/ω, and interaction strength V_0/ω. To detect long-range correlations we define the order parameter

$$q = \left\langle \left| \sum_i (-1)^{x_i + y_i} \hat{\sigma}_{ee}^{(i)} \right| \right\rangle \Big/ \left\langle \sum_i \hat{\sigma}_{ee}^{(i)} \right\rangle. \quad (4)$$

As illustrated in Fig. 1, q measures the population imbalance on the two sublattices reflecting checkerboard ordering, with $q > 0$ in the ordered phase and $q = 0$ in the disordered phase.

If the Rydberg-Rydberg interaction is approximated by a NN blockade, the above model is analytically solvable, showing that long-range order cannot occur in 1D. In higher
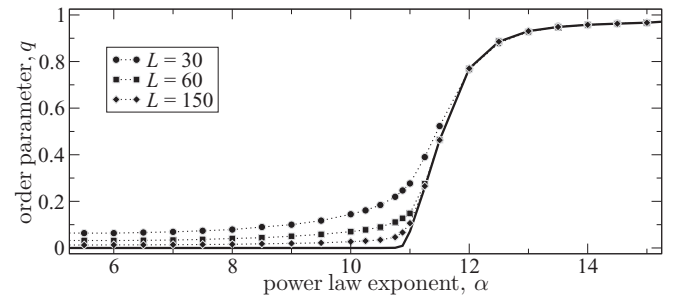

FIG. 2. Order parameter as a function of the power-law exponent α, for $p_0 = 0.95$ and $V_0 = 5\omega$ and resonant driving $\Delta = 0$. The symbols show results for finite system sizes given in the legend. The thick solid line shows the extrapolation to the thermodynamic limit, $L \to \infty$. Finite-size scaling shows a linear increase of the order parameter in the critical regime (exponent: 1 ± 0.05).

dimensions, the steady state exhibits Néel order provided that $p_0 \gtrsim 0.7914$ in two-dimensional (2D) and $p_0 \gtrsim 0.749$ in three-dimensional (3D) square lattices [25]. For simple two-level driving, $p_0 \leqslant 0.5$, and thus crystallization is not possible in any dimension.

In order to clarify the significance of the NN approximation, we have performed ssMC simulations for resonantly driven atoms and varying exponents α, for $p_0 = 0.95$, giving crystallization under the NN-blockade assumption. As shown in Fig. 2, the NN approximation fails qualitatively for the important case of vdW interactions ($\alpha = 6$), which does not support long-range order. Surprisingly, the weak tail of the interactions prevents crystallization until $\alpha \approx 11$. In fact, the simulations show that resonantly driven atoms, with vdW interactions, remain in the disordered phase for any values of p_0 and V_0. It is interesting to note that the order parameter increases linearly with the exponent α in the critical regime.

Long-range order can, however, be stabilized via a finite laser detuning Δ. This is demonstrated in Fig. 3, showing the order parameter q for finite detunings and a varying p_0 and V_0. As shown in Fig. 3(a), Néel-type ordering indeed emerges within a finite detuning range and for $p_0 > p_c \approx 0.86$, only slightly larger than the threshold in the NN-blockade model [25]. Yet, Néel states are only found in a certain interval of interaction strengths V_0, since the vdW tail prevents long-range ordering beyond a critical value [Fig. 3(b)].

The location of the transition can be understood as follows: A Néel state is characterized by a macroscopic population imbalance on the two sublattices with lattice constant $\sqrt{2}a$. Assuming that an atom on the highly populated sublattice has an average of z nearest neighbors, the laser detuning must compensate the corresponding level shifts such that its excitation probability remains above threshold, i.e., $\bar{\rho}_i(\Delta/\omega - zV_0/8\omega) \geqslant p_c$, with $\bar{\rho}_i$ given by Eq. (3) and $z \approx 3$ near the crystallization transition. The parameter region where this condition is fulfilled is marked in Fig. 3 and qualitatively reproduces our numerical results.

Figure 3(c) shows the order parameter as a function of Δ in the thermodynamic limit, indicating second-order phase transitions between the AF and paramagnetic phase. In order to quantitatively assess the importance of fluctuations and the shape of the interaction potential, Fig. 3(c) also gives a
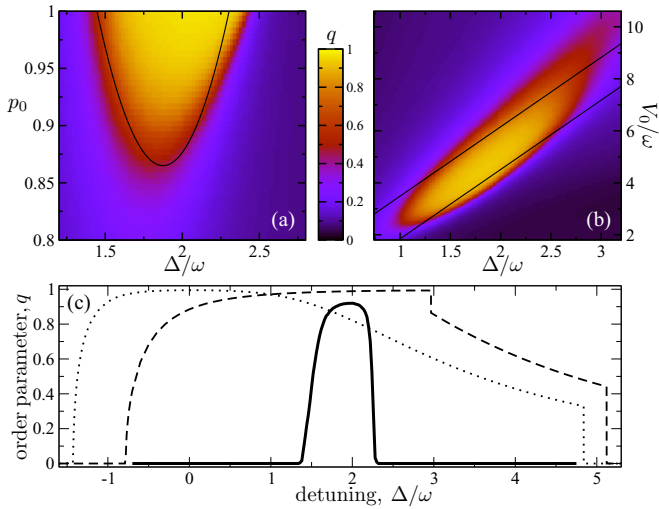
FIG. 3. (Color online) Order parameter obtained for a 30×30 lattice as a function of (a) Δ and p_0 for $V_0 = 5\omega$ and (b) Δ and V_0 for $p_0 = 0.96$. The dashed line shows an estimate of the phase boundary (see text). (c) shows the order parameter after finite-size scaling for $p_0 = 0.96$ and $V_0 = 5\omega$ (solid line) compared to mean-field predictions for NN interactions (dotted line) and the full vdW interactions (dashed line).

comparison to mean-field results under the NN approximation [8,16] and for full vdW interactions. Both cases give qualitatively different predictions, suggesting Néel order at negative detunings and a first-order transition to the reentrant paramagnet at $\Delta > 0$.

To characterize the phase transition we now discuss its static and dynamic properties. The ordered phase with $q \neq 0$ is associated with nondecaying spin-spin correlations, whereas they fall off exponentially on a length scale ξ outside this phase. The inverse correlation length extracted from spin-spin correlation functions in Fig. 4(a) illustrates this behavior and allows the determination of the critical scaling at the phase transition. For the nonequilibrium transition discussed here the static exponent is $\nu \approx 1$, which agrees with the value found for the equilibrium Ising model in two dimensions. A continuous transition to a phase with long-range order is usually associated with a critical slowdown, and the same has been found for free dissipative lattice models [26–28].
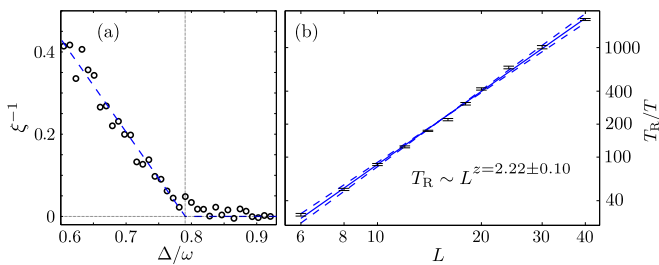

FIG. 4. (Color online) (a) Finite-size extrapolation of the inverse correlation length ξ^{-1} near the phase transition at $\Delta = \Delta_c \approx 0.79\omega$ for $\alpha = 6$, $p_0 = 0.9$, $V_0/\omega = 2.97$. The dashed line corresponds to $\xi^{-1} \propto |\Delta - \Delta_c|^1$. (b) Scaling of relaxation time with the linear size of the two-dimensional system for parameters as in (a) and $\Delta = \omega$ within the ordered phase.

Using dMC we have access to the full time evolution and we extract the relaxation time from the asymptotic approach of the Néel order parameter to its steady-state value. The scaling of this relaxation time defines the dynamical critical exponent of the model, which we find to be $z = 2.22 \pm 0.10$, as shown in Fig. 4(b). This value is compatible with results for kinetic Ising models, notably without a power-law interaction [29,30]. The observed dynamical properties are very similar to those of "model A" in the classification scheme of equilibrium critical dynamics of Hohenberg and Halperin [9].

The effects of power-law interactions as well as of the dissipative nature of the phase transition can be illuminated by direct comparison of the steady state $\bar{\rho}$ of Eq. (2) to the corresponding equilibrium state. In the limit $\alpha \to \infty$, the rate equations fulfill detailed balance conditions and $\bar{\rho}$ coincides with the thermal equilibrium of a corresponding Ising model

$$\rho_{\text{Is}} = \frac{1}{Z} \exp\left\{ -\beta\left[h \sum_j \hat{\sigma}_j^z \right.\right.$$
$$\left.\left. + \sum_{i<j} V_{i,j}\left(\hat{\sigma}_i^z + \frac{1}{2}\right)\left(\hat{\sigma}_j^z + \frac{1}{2}\right) \right] \right\}, \qquad (5)$$

where $\hat{\sigma}_i^z = \hat{\sigma}_{\text{ee}}^{(i)} - 1/2$, if $V_{i,j} \to \infty$ for next neighbors and zero otherwise, and $\beta h = \ln \frac{1-p_0}{p_0}$. Such a correspondence no longer holds in the case of power-law interactions for which one can easily show that the rate equations do not satisfy a detailed balance. We demonstrate this by calculating the minimum trace norm distance $\mathcal{F}$ between the nonequilibrium steady state and the thermal state of an Ising model. Note that the average distance between two random density matrices is 0.5. We optimized the corresponding parameters in Eq. (5) such as the external field h and allow for NN and NNN couplings to minimize $\mathcal{F}$, but found no good agreement, as can be seen in Fig. 5. Thus while the universal properties, characterized by static and dynamic critical exponents, are in agreement with those of the classical Ising model, the specific state is not reproduced by a thermal state.

We finally discuss two experimental implementations of the described system that overcome the two-level limit of $p_0 \leqslant 0.5$. Consider first a lattice of small atomic clouds,
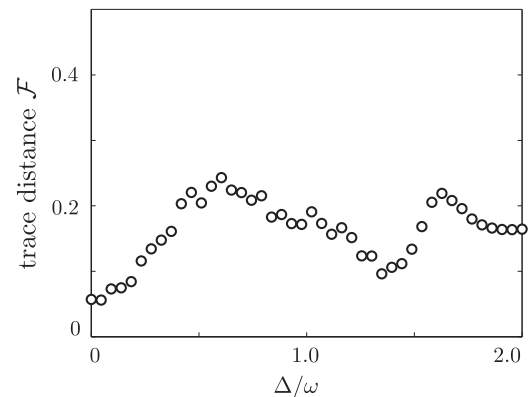

FIG. 5. Trace norm distance $\mathcal{F}$ of the steady state to a thermal state of an Ising model with optimized values of β, h, and V_{ij} [cf. Eq. (5)] for a 4×4 lattice with periodic boundary conditions and $\alpha = 6$, $p_0 = 0.9$, $V_0/\omega = 2.97$.

each containing N two-level atoms. Here $\hat{H}_i = \Omega \hat{\sigma}_{eg}^{(i)} + \text{H.c.}$ couples directly the ground and Rydberg state, which decays with a spontaneous decay rate γ. For sufficiently strong interactions, the blockade inhibits multiple Rydberg excitations within the cloud, such that each site acts as an effective two-level "superatom" [31,32] composed of the collective ground state $|G\rangle$ and the symmetric, singly excited state $|E_0\rangle$ with an enhanced Rabi frequency $\sqrt{N}\Omega$. Additional single-atom dephasing with a rate γ_d transfers population between $|E_0\rangle$ and the manifold of $N-1$ singly excited, nonsymmetric states $|E_k\rangle$ [33] Fig. 1(d). In the limit of strong dephasing, adiabatic elimination yields classical rates $\Gamma_{\uparrow(\downarrow)}$ for transitions between $|G\rangle$ and the manifold of singly excited states. The steady-state excitation probability is given by Eq. (3) with $p_0 = N/[N(1 + \gamma/\bar{\gamma}) + \gamma_d/\bar{\gamma} + \gamma \bar{\gamma}/(4\Omega^2)]$, where $\bar{\gamma} = \gamma + \gamma_d$. For large N, $p_0 \to 1/(1 + \gamma/\bar{\gamma} + 1/N)$, which approaches unity for strong dephasing [33] and $\omega = \sqrt{N}\Omega\sqrt{\gamma_d/\gamma}$. The described superatom lattices can be realized with magnetic or optical microtrap arrays [34–36] that accommodate $N \approx 10 \ldots 100$ atoms per site and provide lattice constants of a few μm for which strong NN interactions can be obtained.

Alternatively, p_0 can be controlled on a single-atom level using three-level excitation via a low-lying intermediate state $|p\rangle$ with two Rabi frequencies Ω_1 and Ω_2 [Fig. 1(c)]. Here, the fast decay of the intermediate state with a rate $\gamma \sim$ MHz drives the relaxation towards the steady state, Eq. (3), with a tunable $p_0 = \Omega_1^2/(\Omega_1^2 + \Omega_2^2)$. Such three-level excitation schemes are utilized in numerous Rydberg atom experiments, either exploring interaction effects in the strong excitation regime $(\Omega_1 > \Omega_2)$ [37–40] or quantum optics applications in the opposite limit [41–44]. As a specific example, laser excitation of Rb $(35S_{1/2})$ Rydberg states via the intermediate Rb $(5P_{1/2})$ state with $\Omega_1 = 0.5\gamma = 4\Omega_2$ yields $p_0 \approx 0.9$, upon accounting for the small but non-negligible Rydberg state decay. For a lattice constant of $a \approx 2$ μm these conditions correspond to $V_0 \approx 5\omega$, i.e., well within the parameter region of the ordered phase. Rydberg excitation and trapping [45] as well as site-resolved Rydberg atom imaging [46] have been experimentally demonstrated in 2D lattices with $a \approx 0.5$ μm. Larger lattice constants can also be realized in these settings [47] or via optical microtrap arrays [48], such that the creation

and probing of the predicted dissipative phase transition appear to be well within experimental reach. Moreover, such experiments could shed light on the transition to the moderate-to-weak damping regime, either via stronger laser driving or employing narrow transitions, e.g., using two-photon Rydberg excitation of two-electron atoms [49] via narrow intermediate states [50].

In conclusion, we have shown that Rydberg lattices can undergo a dissipative phase transition to a long-range-ordered AF phase. A key requirement is the use of optical coupling schemes that go beyond the inversion limit of simple two-level driving and a finite laser detuning to counteract the effects of the power-law tail of the interaction potential. While we have focused here on neutral-atom settings with *finite-range* vdW interactions $(\alpha = 6)$, effective quantum magnets with variable power-law interactions [51] are currently attracting great interest in the context of laser-cooled ion crystals in which various spin models [52] with $\alpha = 0 \ldots 3$ can be realized in one and two dimensions [53–55]. These systems inherently feature dissipation [56] and thus provide an interesting platform to explore the dissipative phase transition in the nonequilibrium steady state also in the *long-range* interaction regime. In light of the demonstrated failure of mean-field approximations, it would further be of great interest to investigate other dissipative phase transitions predicted by mean-field theory [13]. The critical exponents of the steady-state phase transition were found to fall into the Ising universality class, despite marked differences in the steady states from an Ising model in thermal equilibrium. Finally we have addressed here the limit of strong decoherence, and understanding the transition behavior to weakly damped, strongly interacting quantum many-body systems poses another challenging and likewise important issue for future work.

[1] I. Bloch, J. Dalibard, and W. Zwerger, Rev. Mod. Phys. **80**, 885 (2008).

[2] T. Gericke *et al.*, Nat. Phys. **4**, 949 (2008); N. Gemelke *et al.*, Nature (London) **460**, 995 (2009); J. F. Sherson *et al.*, *ibid.* **467**, 68 (2010); W. S. Bakr *et al.*, Science **329**, 547 (2010).

[3] M. Saffman, T. G. Walker, and K. Molmer, Rev. Mod. Phys. **82**, 2313 (2010).

[4] T. Lahaye, C. Menotti, L. Santos, M. Lewenstein, and T. Pfau, Rep. Prog. Phys. **72**, 126401 (2009).

[5] T. Pohl, E. Demler, and M. D. Lukin, Phys. Rev. Lett. **104**, 043002 (2010).

[6] J. Schachenmayer, I. Lesanovsky, A. Micheli, and A. J. Daley, New J. Phys. **12**, 103044 (2010).

[7] R. M. W. van Bijnen *et al.*, J. Phys. B **44**, 184008 (2011).

[8] T. E. Lee, H. Häffner, and M. C. Cross, Phys. Rev. A **84**, 031402 (2011).

[9] P. C. Hohenberg and B. I. Halperin, Rev. Mod. Phys. **49**, 435 (1977).

[10] S. Diehl, A. Tomadin, A. Micheli, R. Fazio, and P. Zoller, Phys. Rev. Lett. **105**, 015702 (2010).

[11] M. Müller *et al.*, Adv. At. Mol. Opt. Phys. **61**, 1 (2012).

[12] L. M. Sieberer, S. D. Huber, E. Altman, and S. Diehl, Phys. Rev. Lett. **110**, 195301 (2013).

[13] T. E. Lee, S. Gopalakrishnan, and M. D. Lukin, Phys. Rev. Lett. **110**, 257204 (2013).

[14] C. Ates, B. Olmos, J. P. Garrahan, and I. Lesanovsky, Phys. Rev. A **85**, 043620 (2012).

[15] M. Höning, D. Muth, D. Petrosyan, and M. Fleischhauer, Phys. Rev. A **87**, 023401 (2013).

[16] J. Qian, G. Dong, L. Zhou, and W. Zhang, Phys. Rev. A **85**, 065401 (2012).

[17] H. Weimer, R. Löw, T. Pfau, and H. P. Büchler, Phys. Rev. Lett. **101**, 250601 (2008).

[18] S. Ji, C. Ates, and I. Lesanovsky, Phys. Rev. Lett. **107**, 060406 (2011).

[19] C. Ates, T. Pohl, T. Pattard, and J. M. Rost, Phys. Rev. Lett. **98**, 023002 (2007); Phys. Rev. A **76**, 013413 (2007); J. Phys. B **39**, L233 (2006).

[20] C. Ates, S. Sevincli, and T. Pohl, Phys. Rev. A **83**, 041802 (2011).

[21] K. P. Heeg, M. Gärttner, and J. Evers, Phys. Rev. A **86**, 063421 (2012).

[22] I. Lesanovsky and J. P. Garrahan, Phys. Rev. Lett. **111**, 215305 (2013).

[23] D. W. Schönleber, M. Gärttner, and J. Evers, Phys. Rev. A **89**, 033421 (2014).

[24] A. F. Voter, in *Radiation Effects in Solids*, edited by K. E. Sickafus, E. A. Kotomin, and B. P. Uberuaga, NATO Science Series II: Mathematics, Physics and Chemistry (Springer, Berlin, 2007), Vol. 235.

[25] P. Pearce and K. Seaton, J. Stat. Phys. **53**, 1061 (1988).

[26] J. Eisert and T. Prosen, arXiv:1012.5013.

[27] M. Höning, M. Moos, and M. Fleischhauer, Phys. Rev. A **86**, 013606 (2012).

[28] B. Horstmann, J. I. Cirac, and G. Giedke, Phys. Rev. A **87**, 012108 (2013).

[29] E. Stoll, K. Binder, and T. Schneider, Phys. Rev. B **8**, 3266 (1973).

[30] M. P. Nightingale and H. W. J. Blöte, Phys. Rev. Lett. **76**, 4548 (1996).

[31] M. D. Lukin *et al.*, Phys. Rev. Lett. **87**, 037901 (2001).

[32] D. Petrosyan, M. Höning, and M. Fleischhauer, Phys. Rev. A **87**, 053414 (2013).

[33] J. Honer, R. Löw, H. Weimer, T. Pfau, and H. P. Büchler, Phys. Rev. Lett. **107**, 093601 (2011).

[34] J. D. Weinstein and K. G. Libbrecht, Phys. Rev. A **52**, 4004 (1995).

[35] R. Dumke *et al.*, Phys. Rev. Lett. **89**, 097903 (2002).

[36] S. Whitlock, R. Gerritsma, T. Fernholz, and R. J. C. Spreeuw, New J. Phys. **11**, 023021 (2009).

[37] H. Schempp *et al.*, Phys. Rev. Lett. **104**, 173602 (2010); **112**, 013002 (2014).

[38] A. Schwarzkopf, R. E. Sapiro, and G. Raithel, Phys. Rev. Lett. **107**, 103001 (2011); A. Schwarzkopf, D. A. Anderson, N. Thaicharoen, and G. Raithel, Phys. Rev. A **88**, 061406(R) (2013).

[39] J. Nipper *et al.*, Phys. Rev. X **2**, 031011 (2012).

[40] M. Viteau *et al.*, Phys. Rev. Lett. **109**, 053002 (2012).

[41] J. D. Pritchard *et al.*, Phys. Rev. Lett. **105**, 193603 (2010).

[42] Y. O. Dudin and A. Kuzmich, Science **336**, 887 (2012).

[43] T. Peyronel *et al.*, Nature (London) **488**, 57 (2012).

[44] D. Maxwell *et al.*, Phys. Rev. Lett. **110**, 103001 (2013).

[45] S. E. Anderson, K. C. Younge, and G. Raithel, Phys. Rev. Lett. **107**, 263001 (2011).

[46] P. Schauss *et al.*, Nature (London) **491**, 87 (2012).

[47] T. Fukuhara *et al.*, Nature (London) **502**, 76 (2013).

[48] L. Béguin, A. Vernier, R. Chicireanu, T. Lahaye, and A. Browaeys, Phys. Rev. Lett. **110**, 263201 (2013); D. Barredo, S. Ravets, H. Labuhn, L. Béguin, A. Vernier, F. Nogrette, T. Lahaye, and A. Browaeys, *ibid.* **112**, 183002 (2014); F. Nogrette, H. Labuhn, S. Ravets, D. Barredo, L. Béguin, A. Vernier, T. Lahaye, and A. Browaeys, Phys. Rev. X **4**, 021034 (2014).

[49] J. Millen, G. Lochead, and M. P. A. Jones, Phys. Rev. Lett. **105**, 213004 (2010).

[50] L. I. R. Gil, R. Mukherjee, E. M. Bridge, M. P. A. Jones, and T. Pohl, Phys. Rev. Lett. **112**, 103601 (2014).

[51] J. Schachenmayer, B. P. Lanyon, C. F. Roos, and A. J. Daley, Phys. Rev. X **3**, 031015 (2013).

[52] D. Porras and J. I. Cirac, Phys. Rev. Lett. **92**, 207901 (2004).

[53] J. W. Britton *et al.*, Nature (London) **484**, 489 (2012).

[54] R. Islam *et al.*, Science **340**, 583 (2013).

[55] P. Richerme *et al.*, Nature **511**, 198 (2014); P. Jurcevic, B. P. Lanyon, P. Hauke, C. Hempel, P. Zoller, R. Blatt, and C. F. Roos, *ibid.* **511**, 202 (2014).

[56] M. Foss-Feig, K. R. A. Hazzard, J. J. Bollinger, and A. M. Rey, Phys. Rev. A **87**, 042101 (2013); New J. Phys. **15**, 113008 (2013).